ROUNDED TRIANGULAR BILLIARDS

CARL P. DETTMANN

Abstract. Fifty years ago, Leonid Bunimovich showed that convex billiards could be hyperbolic, using billiards where the boundary consists of straight segments and circular arcs such that the disks defined by the arcs are contained in the billiard. Two well known examples with C^1 boundaries, the straight and tilted stadia, have families of neutral periodic orbits, and hence are not fully hyperbolic. We present the parameter space of the fully hyperbolic Bunimovich billiards formed by rounding the corners of the three integrable triangular billards. By construction these have C^1 boundaries and are convex.

1. Introduction

Fifty years ago, Leonid Bunimovich showed that convex billiards could be hyperbolic [4]. He considered a class of billiards now known as Bunimovich billiards with boundaries consisting of straight lines and circular arcs such that each disk is strictly contained in the billiard (the "B-condition"). In fact, the disk inclusion may be replaced by the condition that the interval between successive collisions with circular arcs is at least that of the relevant chord [5, 15], and (for non-convex geometries) dispersing components, that is, concave components or convex obstacles with nowhere zero curvature, are allowed [3, 12, 15]. Other classes of chaotic billiards, generalising the circular arcs to curves now called absolutely focusing, have been shown to be hyperbolic [7, 18, 22, 28, 32]. Here we construct billiards using circular arcs, but it would also be possible to use more general absolutely focusing arcs, sufficiently separated.

Two very well known Bunimovich billiards are the straight stadium [1], with two parallel straight sides and semicircular arcs, Fig. 1(a), and the tilted stadium [20], with two straight but nonparallel sides, and two arcs, one less than 180° and one greater than 180°, Fig. 1(b). In each case almost all trajectories reach both straight and curved components and hence are hyperbolic, but there are families of nonhyperbolic period two orbits, in the straight stadium between the parallel sides, and in the tilted stadium as diameters of the larger arc. The first Bunimovich billiard [8], also with non-hyperbolic periodic two orbits, was the truncated circle with an arc of

Date: October 10, 2024.

2020 *Mathematics Subject Classification.* 37C83, 37D40.

Key words and phrases. billiards, hyperbolicity.

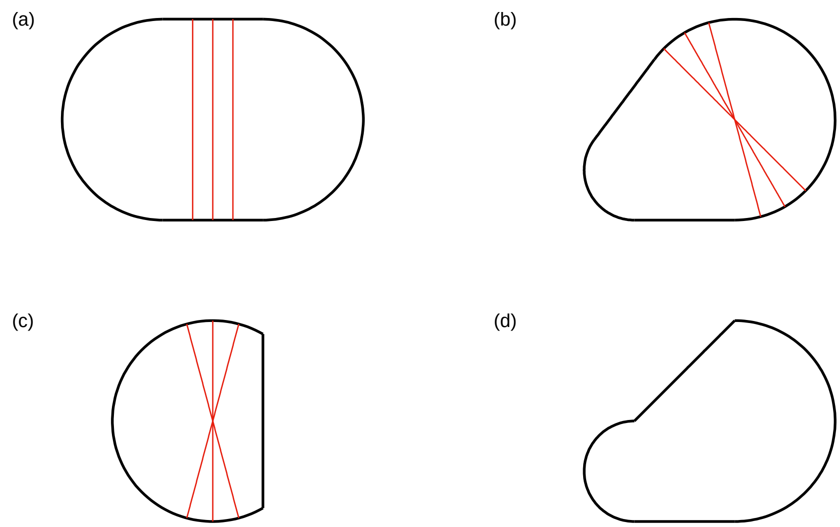

FIGURE 1. (a) Straight stadium. (b) Tilted stadium. (c) Truncated circle. (d) C^0 stadium. Each of these is formed from straight line segments and circular arcs. The thin lines in (a,b,c) are non-hyperbolic periodic orbits.

greater than 180°, Fig. 1(c), however unlike the (C^1) stadia, it has only C^0 smoothness.

Here, we seek billiard geometries that are fully hyperbolic, that is, do not contain any nonhyperbolic orbits. Because they are convex, they do not contain grazing collisions either. There are in any Bunimovich billiard sliding orbits with many collisions on a single circular arc. However these exist only for bounded continuous time, so whilst affecting the statistical properties of the billiard map, they may allow strong properties, perhaps exponential decay of correlations, for the flow.

Convex billiards without straight sides, and hence not satisfying the B-condition, have also been considered. The asymmetric lemon, a C^0 convex billiard with two circular arcs, has been proved hyperbolic under some technical conditions [13]. Ref. [2] considers a family of C^1 convex billiards with four circular arcs. The authors discuss elliptic islands surrounding periodic orbits for much of the parameter space, but also conjecture (with numerical evidence) that close to the limit of tilted stadia, where two opposite arcs become straight, the dynamics is ergodic. For both Refs. [2] and [13] it is possible that some parameters with all arcs less than 180° are fully hyperbolic. More recently, the case of many circular arcs has been considered rigorously, showing properties characteristic of hyperbolicity, but on subsets of phase space [17]. Beyond circular arcs, it is known that sufficiently smooth (C^6) boundaries of convex billiard lead to caustics accumulating at the boundary and hence are not fully hyperbolic [23]. However, boundaries should be comprised of a finite number of sufficiently smooth (C^3) components to avoid collisions accumulating in finite time [26].

One billiard with fully hyperbolic dynamics is that of a stadium with two semicircles and straight sides that are not parallel and long enough that the larger circle is contained in the billiard if the latter is reflected across its straight sides, Fig. 1(d). However, this example has only C^0 boundaries, so that the dynamics cannot be continued for a trajectory that reaches a corner. For this reason, and also to avoid corner effects in both the classical and quantum dynamics, we now require C^1 smoothness, as with the straight and tilted stadia, and the highest possible for boundaries comprised of both straight sides and circular arcs.

It is not possible for a Bunimovich billiard to be convex, C^1 and fully hyperbolic with fewer than three straight sides. Zero sides is the integrable circular billiard, one side is the truncated circle, and two sides are the straight and tilted stadia. Here we consider the case of three straight sides, the rounded triangles, and give the parameter regions for which the rounded integrable right triangles satisfying the B-condition are fully hyperbolic. We also show that rounded integrable quadrilaterals satisfying the B-condition are never fully hyperbolic.

The use of integrable polygons is only to simplify the analysis of the billiard orbits. There are many rounded polygons where either a proof that all orbits touch a curved component, or a proof that there is a periodic orbit that does not touch the curved component, is a finite computation. These include perturbations of the examples given here, so form a positive measure set of parameters.

It is not known whether all general polygonal (even triangular) billiards contain a periodic orbit [30]. Each non-periodic orbit does however accumulate to at least one corner [24], which allowed Chernov and Troubetzkoy [16] to conclude for convex polygons with all corners rounded that orbits avoiding the curved components form a countable union of periodic strips (continuous families of periodic orbits), improved in Ref. [19] to a finite union. In our examples the set avoiding curved components is in fact empty. If the B-condition is satisfied (as in our case), convex polygons with all corners rounded are ergodic, as shown in Ref. [16] using results from Refs. [11, 12, 14]; see also Refs. [6, 31].

In the future it would be good to know the extent to which the B-condition could be relaxed whilst retaining full hyperbolicity, similar to the lemon billiard mentioned above. The three dimensional case is more challenging, with astigmatism effects [10]. Known examples of proved [9] and numerical [25] convex hyperbolic three dimensional billiards have non-hyperbolic orbits, making quantum analysis more difficult [21]. Are there convex three dimensional billiards (C^0 or C^1) that are fully hyperbolic? In two dimensions at least, quantum chaos can now be considered without the complications of C^0 corners and non-hyperbolic orbits. Are rounded triangular billiards quantum unique ergodic [27]?

Acknowledgements

This work is in celebration of the 75th birthday of Leonid Bunimovich. The idea for seeking C^1 fully hyperbolic billiards came around 2009 from an experimental physicist. The author is also grateful for helpful discussions with David Phillips, whose undergraduate project report [29] contains many ideas used herein, and also Domokos Szász and Serge Troubetzkoy.

2. Definitions

Angles are measured in degrees. Polygonal billiards where all angles are of the form $\frac{180°}{n}$ can be unfolded to $\mathbb{R}^2$, where their orbits are straight lines. These are termed integrable (polygonal) billiards. They are the rectangle (including square), 60-60-60 triangle, 45-45-90 triangle and 30-60-90 triangle.

Here, we replace the corners of an integrable billiard by circular arcs tangent to the sides of the polygon. The Bunimovich condition (B-condition see Refs. [4, 12]) is that the disks formed by continuing the circular arcs are contained in the billiard, and is sufficient for hyperbolicity. For the integrable billiards, the B-condition is equivalent to the requirement that the radius of the arcs are all less than or equal to that of the incircle. Clearly, there is a trivial exception in that if the resulting billiard is a disk it is not hyperbolic. The rounded integrable billiards are depicted in Fig. 2.

We defer the case of quadrilaterals to Sec. 3 and only refer to integrable triangles for the remainder of this section. We define the length of the longest side to be 1. We label the vertices A, B, C in order of increasing angle $\theta_a \leq \theta_b \leq \theta_c$, and set a, b and c to be the distance from the relevant corner of the triangle to the intersection of the arc with the side of the triangle. Thus the radius of the arc at A is $a \tan \frac{\theta_a}{2}$. Without loss of generality, we take $a \geq b$ in the 45-45-90 triangle and $a \geq b \geq c$ in the 60-60-60 triangle.

The B-condition is

$$v \tan \frac{\theta_v}{2} \leq r_{in} \qquad \forall v \in \{a, b, c\} \tag{2.1}$$

where r_{in} is the inradius of the triangle. We denote the strict version of this as the strict B-condition. In the case of equality, we refer to the arc as maximal.

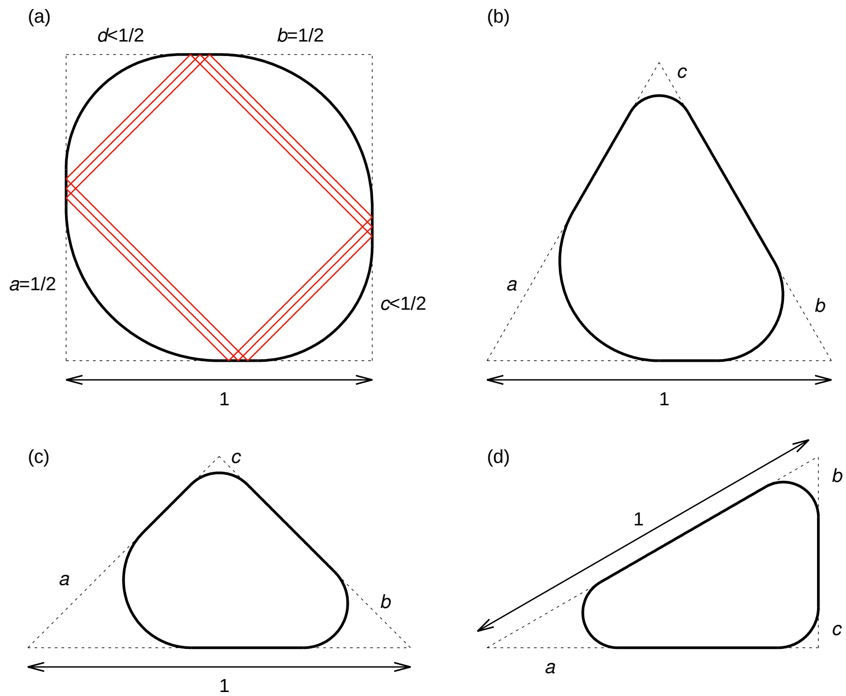

FIGURE 2. Rounded integrable polygons: (a) Square (b) 60-60-60 triangle (c) 45-45-90 triangle (d) 30-60-90 triangle. For the rectangle, see Fig. 1(a). Each of these is formed from straight line segments and circular arcs. The thin lines in (a) are non-hyperbolic periodic orbits. The others are fully hyperbolic.

Since none of the arcs have radius larger than the incircle, they also cannot intersect, except possibly at their endpoints. All (including nonintegrable) rounded triangles satisfying Eq. (2.1) are Bunimovich billiards, and hence are hyperbolic, except where all three arcs are maximal leading to a circular billiard. Also, if two arcs are maximal, the result is a tilted stadium, Fig. 1(b), and not fully hyperbolic. Thus for a Bunimovich billiard to be fully hyperbolic, at most one arc can be maximal, and the others satisfy the strict B-condition. The parameter space of fully hyperbolic Bunimovich billiards is thus partitioned

$$\mathcal{P} = \mathcal{P}_0 \cup \mathcal{P}_A \cup \mathcal{P}_B \cup \mathcal{P}_C \subset \mathbb{R}^3 \tag{2.2}$$

where $\mathcal{P}_0$ is the set of $\{a, b, c\}$ where each arc satisfies the strict B-condition and $\mathcal{P}_V$ for $V \in \{A, B, C\}$ is the set where the V arc is maximal and the others satisfy the strict B-condition, and in all cases the billiard is fully hyperbolic.

A rounded integrable billiard is fully hyperbolic if and only if when unfolded to $\mathbb{R}^2$ there are no infinite trajectories that avoid a curved component ("finite horizon condition"). Trajectories that touch the boundary of curved components have singular derivatives as the boundary is only C^1, and those for which all nearby trajectories reach the interior of the boundary components are allowed in fully hyperbolic billiards.

Unfolding each of the curved right angled triangles leads to a lattice of stars, see Figs. 3, 4, 5 below. The star corresponding to a vertex of angle θ_v has $\frac{360^\circ}{\theta_v}$ points. We refer to the stars using the relevant vertex, eg A-star.

For each lattice of extended obstacles, there are only a finite number (including zero) of directions in which there are infinite straight line trajectories that avoid the obstacles. For a lattice of stars, to show that a direction is blocked, we may replace the stars by disks given by the incircles of their convex hulls. The convex hull of a V-star (for $V \in \{A, B, C\}$) is a regular $\frac{360^\circ}{\theta_v}$-gon of circumradius v and inradius $v \cos \frac{\theta_v}{2}$. Then we apply the following elementary proposition:

Proposition 2.1. *Consider the square (respectively, triangular) lattice, with lattice spacing d, and disks of radius r. The direction defined by a primitive lattice vector, that is, by coprime integers (m, n) with length $d\sqrt{m^2+n^2}$ (respectively, $d\sqrt{m^2+mn+n^2}$), is blocked if $r > \frac{d}{2\sqrt{m^2+n^2}}$ (respectively, $r > \frac{d\sqrt{3}}{4\sqrt{m^2+mn+n^2}}$).*

The shortest primitive lattice vectors have $m^2 + n^2 \in \{1, 2, 5, 10, \ldots\}$ for the square lattice and $m^2 + mn + n^2 \in \{1, 3, 7, 13, \ldots\}$ for the triangular lattice.

In the remaining sections we deal with each of the integrable billiards in turn, the quadrilaterals in Sec. 3, the 60-60-60 triangle in Sec. 4, the 45-45-90 triangle in Sec. 5 and the 30-60-90 triangle in Sec. 6, deriving the set $\mathcal{P}$ for each case. The results include some cases where $c = 0$ in which case only two vertices are rounded and the billiard is C^0 but still fully hyperbolic.

3. Quadrilaterals

For quadrilaterals, a maximal arc touches the midpoint of the shorter side.

Theorem 3.1. *Rounded integrable quadrilaterals satisfying the B-condition are not fully hyperbolic.*

Proof. The rectangle has a family of nonhyperbolic periodic orbits, even when all arcs are maximal, as with the straight stadium, Fig 1(a).

For the square, we enumerate the possibilities regarding maximal arcs. If all corners have maximal arcs, the billiard is a disk and not hyperbolic. If three corners have maximal arcs, the billiard is a tilted stadium and not fully hyperbolic, Fig. 1(b). If two horizontally adjacent corners have nonmaximal arcs, there is a horizontal family of nonhyperbolic orbits between these arcs and the horizontal line through the centre of the square, and similarly for vertically adjacent corners. The remaining case, that of two diagonally opposite maximal arcs, has a diagonal family of nonhyperbolic orbits, depicted in Fig. 2(a). □

4. The 60-60-60 triangle

For the rounded 60-60-60 triangle we may assume without loss of generality

$$a \geq b \geq c \tag{4.1}$$

In this section we show

Theorem 4.1. *For the rounded 60-60-60 triangle,*

$$\begin{aligned}\mathcal{P} &= \mathcal{P}_A \\ &= \left\{(a,b,c) : a = \frac{1}{2}, \frac{1}{4} \leq b < \frac{1}{2}, \frac{1}{2} - b \leq c \leq b\right\}\end{aligned} \tag{4.2}$$

Proof. The unfolding of the 60-60-60 triangle with vertices $A(0,0)$, $B(1,0)$, $C(\frac{1}{2}, \frac{\sqrt{3}}{2})$ is shown in Fig. 3. We label trajectories (m,n) with respect to the basis $\{(\frac{3}{2}, \frac{\sqrt{3}}{2}), (\sqrt{3}, 0),\}$ of the A-star lattice. The length of a lattice vector is $d\sqrt{m^2 + mn + n^2}$ where $d = \sqrt{3}$ is the lattice spacing.

The inradius $r_{in} = \frac{\sqrt{3}}{6}$, so that the B-condition Eq. (2.1) becomes

$$a \leq \frac{1}{2} \tag{4.3}$$

We require that all trajectories touch a curved component. A trajectory that avoids all curved components must lie along a lattice vector. As seen in Fig. 3 the $(0,1)$ trajectory requires

$$b + c \geq \frac{1}{2} \tag{4.4}$$

and the $(2,-1)$ trajectory requires

$$a \geq \frac{1}{2} \tag{4.5}$$

The solution of Eqs (4.1,4.3–4.5) with at most one maximal arc is the set Eq. (4.2) as claimed.

We now show that no other directions are relevant using Prop. 2.1. The A-stars form a triangular lattice with spacing $d = \sqrt{3}$. The inradius of the convex hull of the A-stars is $r = \frac{1}{2}\cos 30° = \frac{\sqrt{3}}{4}$. All directions with

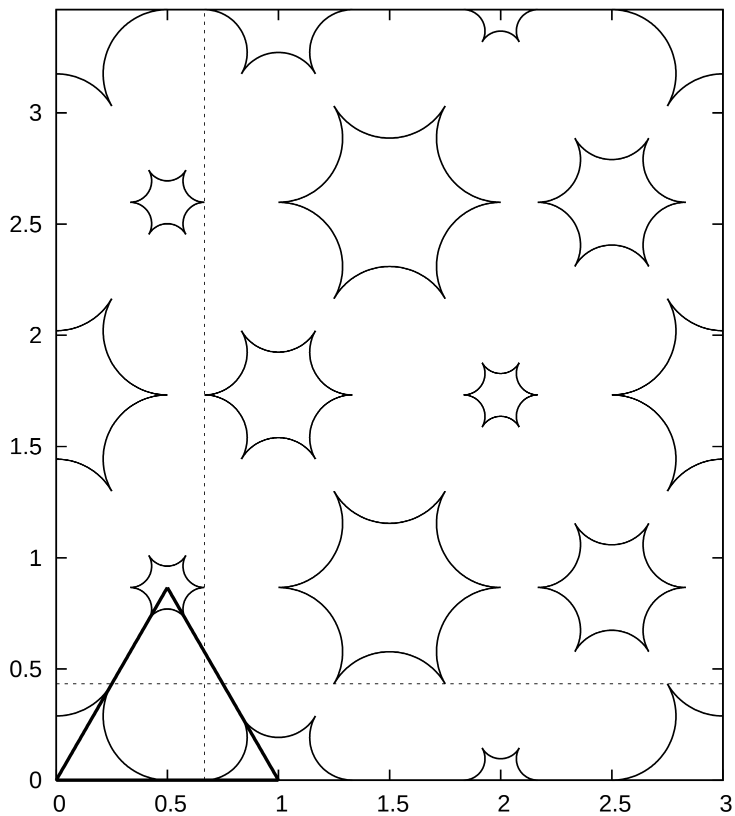

FIGURE 3. Unfolding of the 60-60-60 triangle shown in Fig. 2(b). The A-stars of radius $a = 0.5$, B-stars of radius $b = 0.333$ and C-stars of radius $c = 0.167$ each have six points. The trajectories shown have lattice vectors $(0, 1)$ (vertical) and $(2, -1)$ (horizontal).

$m^2 + mn + n^2 \leq 3$ are equivalent to those considered above, and for $m^2 + mn + n^2 \geq 7$ we have

$$\frac{d\sqrt{3}}{4\sqrt{m^2 + mn + n^2}} \leq \frac{3}{4\sqrt{7}} = 0.283 \ldots < 0.433 \ldots = \frac{\sqrt{3}}{4} \tag{4.6}$$

□

5. The 45-45-90 triangle

For the rounded 45-45-90 triangle we may assume without loss of generality

$$a \geq b \tag{5.1}$$

In this section we show

Theorem 5.1. *For the rounded 45-45-90 triangle,*

(5.2)

$$\mathcal{P} = \mathcal{P}_0 \cup \mathcal{P}_A \cup \mathcal{P}_C$$
$$\mathcal{P}_0 = \left\{ (a,b,c) : \frac{\sqrt{2}}{4} < a < \frac{1}{2}, \frac{\sqrt{2}}{2} - a \leq b \leq a, \frac{\sqrt{2}}{2}(1-2a) \leq c < \frac{\sqrt{2}-1}{2} \right\}$$
$$\mathcal{P}_A = \left\{ (a,b,c) : a = \frac{1}{2}, \frac{\sqrt{2}-1}{2} \leq b < \frac{1}{2}, 0 \leq c < \frac{\sqrt{2}-1}{2} \right\}$$
$$\mathcal{P}_C = \left\{ (a,b,c) : \frac{\sqrt{2}}{4} \leq a < \frac{1}{2}, \frac{\sqrt{2}}{2} - a \leq b \leq a, c = \frac{\sqrt{2}-1}{2} \right\}$$

Proof. The unfolding of the rounded 45-45-90 triangle with vertices $A(0,0)$, $B(1,0)$, $C(1/2,1/2)$ is shown in Fig. 4. We label trajectories (m,n) with respect to the (usual) basis $\{(1,0),(0,1)\}$.

The inradius $r_{in} = \frac{\sqrt{2}-1}{2}$, so that the B-condition Eq. (2.1) becomes

$$b \leq a \leq \frac{1}{2}, \qquad c \leq \frac{\sqrt{2}-1}{2} \approx 0.207 \tag{5.3}$$

As in Sec. 4 a trajectory that avoids all curved components must lie along a lattice vector. As seen in Fig. 4 the $(1,0)$ trajectory requires

$$a + \frac{c}{\sqrt{2}} \geq \frac{1}{2} \tag{5.4}$$

and the $(1,1)$ trajectory requires

$$a + b \geq \frac{\sqrt{2}}{2} \tag{5.5}$$

The solution of Eqs (5.1,5.3–5.5) with at most one maximal arc is the set Eq. (5.2) as claimed.

We now show that no other directions are relevant using Prop. 2.1. The A-stars form a square lattice with spacing $d = \sqrt{2}$. The inradius of the convex hull of the A-stars is $r = a\cos 22.5° = a\frac{\sqrt{2+\sqrt{2}}}{2}$. All directions with $m^2+n^2 \leq 2$ are equivalent to those considered above, and for $m^2+n^2 \geq 5$ we have

$$\frac{d}{2\sqrt{m^2+n^2}} \leq \frac{1}{\sqrt{10}} < \frac{\sqrt{2}}{4}\frac{\sqrt{2+\sqrt{2}}}{2} \leq a\frac{\sqrt{2+\sqrt{2}}}{2} \tag{5.6}$$

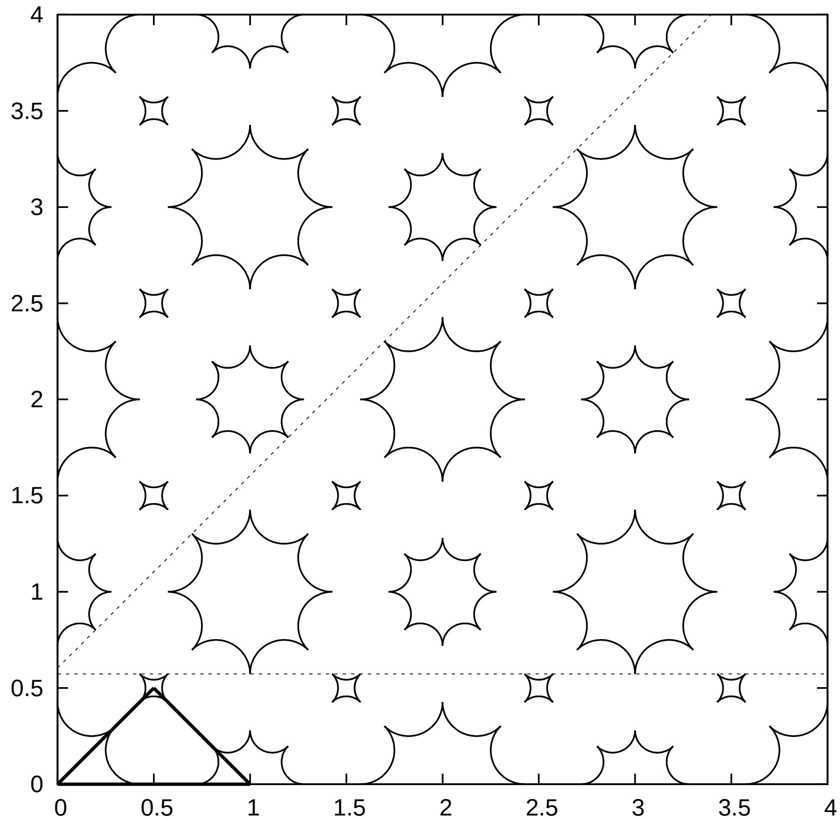

FIGURE 4. Unfolding of the 45-45-90 triangle shown in Fig. 2(c). The A-stars of radius $a = 0.427$ and B-stars of radius $b = 0.280$ have 8 points, while the C-stars of radius $c = 0.104$ have four points. The trajectories shown have lattice vectors $(1, 0)$ (horizontal) and $(1, 1)$ (diagonal).

using the lower bound for a from Eq. (5.2). □

6. The 30-60-90 triangle

In this section we show

Theorem 6.1. *For the rounded 30-60-90 triangle,*

$$
\begin{aligned}
\mathcal{P} =& \mathcal{P}_0 \cup \mathcal{P}_A \cup \mathcal{P}_B \cup \mathcal{P}_C \\
\mathcal{P}_0 =& \Bigg\{ (a,b,c) : \frac{3\sqrt{3}-3}{8} < a < \frac{\sqrt{3}+1}{4}, \\
& \frac{\sqrt{3}-1}{8} < b < \frac{3-\sqrt{3}}{4}, \frac{1}{2} - a \le b, \\
& \max\left(0, \frac{\sqrt{3}-4a}{2\sqrt{3}}, \frac{1-4b}{2\sqrt{3}}\right) \le c < \frac{\sqrt{3}-1}{4} \Bigg\} \\
\mathcal{P}_A =& \Bigg\{ (a,b,c) : a = \frac{\sqrt{3}+1}{4}, \frac{\sqrt{3}-1}{8} < b < \frac{3-\sqrt{3}}{4}, \\
& \max\left(0, \frac{1-4b}{2\sqrt{3}}\right) \le c < \frac{\sqrt{3}-1}{4} \Bigg\} \\
\mathcal{P}_B =& \Bigg\{ (a,b,c) : \frac{3\sqrt{3}-3}{8} < a < \frac{\sqrt{3}+1}{4}, b = \frac{3-\sqrt{3}}{4}, \\
& \max\left(0, \frac{\sqrt{3}-4a}{2\sqrt{3}}\right) \le c < \frac{\sqrt{3}-1}{4} \Bigg\} \\
\mathcal{P}_C =& \Bigg\{ (a,b,c) : \frac{3\sqrt{3}-3}{8} \le a < \frac{\sqrt{3}+1}{4}, \\
& \max\left(\frac{\sqrt{3}-1}{8}, \frac{1}{2} - a\right) \le b < \frac{3-\sqrt{3}}{4}, c = \frac{\sqrt{3}-1}{4} \Bigg\}
\end{aligned}
\tag{6.1}
$$

Proof. The unfolding of the 30-60-90 triangle with vertices $A(0,0)$, $B(\frac{3}{2}, \frac{1}{2})$, $C(\frac{\sqrt{3}}{2}, 0)$ is shown in Fig. 5. We label trajectories (m,n) with respect to the basis $\{(\sqrt{3},0), (\frac{\sqrt{3}}{2}, \frac{3}{2})\}$ of the A-star lattice. The length of a lattice vector is $d\sqrt{m^2+mn+n^2}$ where $d = \sqrt{3}$ is the lattice spacing.

The inradius $r_{in} = \frac{\sqrt{3}-1}{4}$, so that the B-condition Eq. (2.1) becomes

$$
\begin{aligned}
a \le& \frac{\sqrt{3}+1}{4} \approx 0.683 \\
b \le& \frac{3-\sqrt{3}}{4} \approx 0.317 \\
c \le& \frac{\sqrt{3}-1}{4} \approx 0.183
\end{aligned}
\tag{6.2}
$$

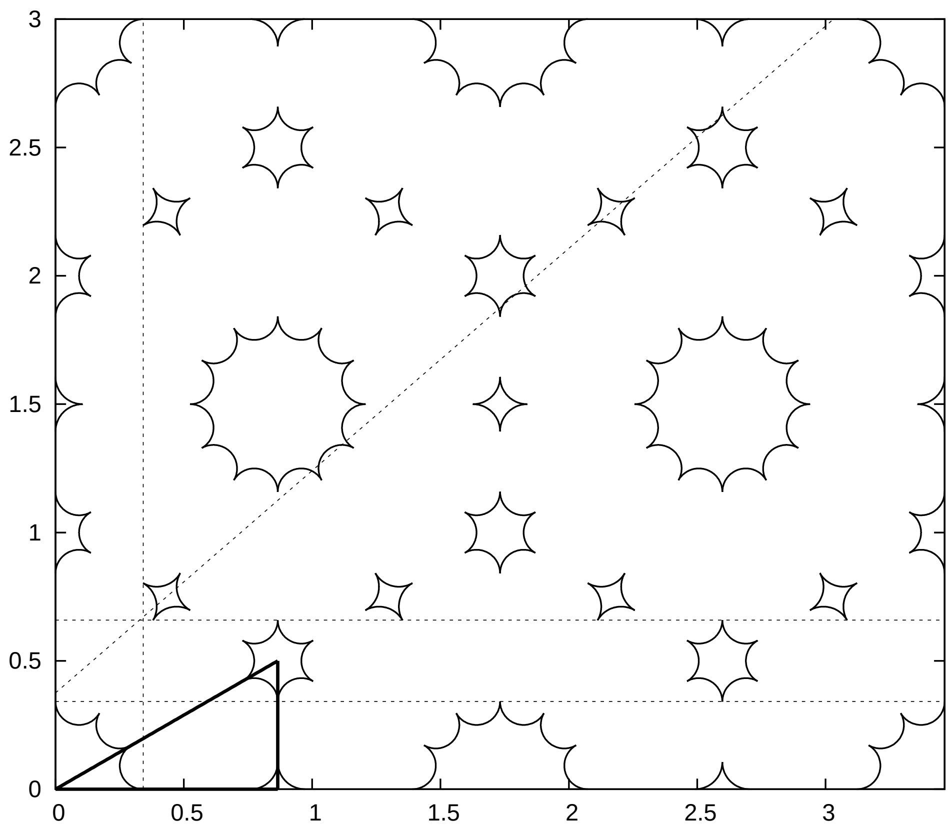

FIGURE 5. Unfolding of the 30-60-90 triangle shown in Fig. 2(d). The A-stars of radius $a = 0.342$ have 12 points, the B-stars of radius $b = 0.159$ have 6 points and the C-stars of radius $c = 0.106$ have 4 points. The trajectories shown have lattice vectors $(1, 0)$ (horizontal), $(-1, 2)$ (vertical), $(1, 2)$ (diagonal).

Trajectories with lattice vector $(1, 0)$ give the inequalities

$$a + b \geq \frac{1}{2}, \qquad b + c\frac{\sqrt{3}}{2} \geq \frac{1}{4} \tag{6.3}$$

Trajectories with lattice vector $(-1, 2)$ give the inequality

$$a + c\frac{\sqrt{3}}{2} \geq \frac{\sqrt{3}}{4} \tag{6.4}$$

The solution set of Eqs (6.2–6.4) with at most one maximal arc is Eq. (6.1) as claimed.

We now show that no other trajectories are relevant. All trajectories (m, n) with $m^2 + mn + n^2 \leq 3$ are equivalent to the above by symmetry. Other trajectories have $m^2 + mn + n^2 \in \{7, 13, \ldots\}$. We apply Prop. 2.1 as before. The A-stars form a triangular lattice with spacing $d = \sqrt{3}$. The inradius of the convex hull of the A-stars is $r = a\cos 15^\circ = a\frac{1+\sqrt{3}}{2\sqrt{2}}$. For $m^2 + mn + n^2 \geq 13$ we have

$$\frac{d\sqrt{3}}{4\sqrt{m^2+mn+n^2}} \leq \frac{3}{4\sqrt{13}} < \frac{3\sqrt{2}}{16} \leq a\frac{1+\sqrt{3}}{2\sqrt{2}} \tag{6.5}$$

using the lower bound for a from Eq. (6.1).

However, the inequality, Eq. (6.5) fails for $m^2 + mn + n^2 = 7$. All such trajectories are equivalent by symmetry to the line $y = \frac{\sqrt{3}}{2}x + \mathcal{C}$ shown in Fig. 5. Now, we use an exact calculation, not approximating by a disk. The A-star at $(0, 0)$ has vertex closest to the line at $a\hat{n}_a$ where $\hat{n}_a = (-\frac{1}{2}, \frac{\sqrt{3}}{2})$, intersecting if $\mathcal{C} < a\frac{3\sqrt{3}}{4}$. The A-star at $(\frac{\sqrt{3}}{2}, \frac{3}{2})$ has vertex closest to the line at $(\frac{\sqrt{3}}{2}, \frac{3}{2}) - a\hat{n}_a$, intersecting if $\mathcal{C} > \frac{3-3\sqrt{3}a}{4}$. These intervals overlap if $a > \frac{\sqrt{3}}{6}$. The B-star at $(\sqrt{3}, 2)$ has vertex closest to the line at $(\sqrt{3}, 2) - b\hat{n}_b$ where $\hat{n}_b = (-\frac{\sqrt{3}}{2}, \frac{1}{2})$, intersecting if $\mathcal{C} > \frac{2-5b}{4}$. The B-star at $(\frac{3\sqrt{3}}{2}, \frac{5}{2})$ has vertex closest to the line at $(\frac{3\sqrt{3}}{2}, \frac{5}{2}) + b\hat{n}_b$, intersecting if $\mathcal{C} < \frac{1+5b}{4}$. These intervals overlap if $b > \frac{1}{10}$. We know from Eq. (6.3) that $a + b > \frac{1}{2}$, thus at least one of $a > \frac{\sqrt{3}}{6}$ and $b > \frac{1}{10}$ is true, and so these trajectories always reach a curved component as required. □

References

[1] P. Bálint, and S. Gouëzel, *Limit theorems in the stadium billiard*, Commun. Math. Phys. **263** (2006), 461–512.

[2] P. Bálint, M. Halász, J. A. Hernández-Tahuilán, and D. P. Sanders, *Chaos and stability in a two-parameter family of convex billiard tables*, Nonlinearity **24** (2011), 1499–1521.

[3] L. A. Bunimovich, *On billiards close to dispersing*, Math. USSR-Sbornik **23** (1974) 45–67.

[4] L. A. Bunimovich, *On ergodic properties of certain billiards*, Func. Anal. Appl. **8** (1974) 254–255.

[5] L. A. Bunimovich, *On the ergodic properties of nowhere dispersing billiards*, Commun. Math. Phys. **65** (1979), 295–312.

[6] L. A. Bunimovich, *A theorem on ergodicity of two-dimensional hyperbolic billiards*, Commun. Math. Phys. **130** (1990), 599–621.

[7] L. A. Bunimovich, *On absolutely focusing mirrors*, In Ergodic Theory and Related Topics III: Proceedings of the International Conference held in Güstrow, Germany, October 22—27, 1990 Springer, Berlin (1992), 62–82.

[8] L. A. Bunimovich, *Chaos and Geometrical Optics*, Radiophysics and Quantum Electronics, **64** (2022) 693–699.

[9] L. A. Bunimovich and G. D. Magno *Semi-focusing billiards: Hyperbolicity*, Commun. Math. Phys. **262** (2006), 17–32.

[10] L. A. Bunimovich, and J. Rehacek, *On the ergodicity of many-dimensional focusing billiards*, Ann. Inst. Henri Poincaré Physique théorique **68** (1998) 421–448.

[11] L. A. Bunimovich, Ya. G. Sinai and N. I. Chernov, *Markov partitions for two-dimensional hyperbolic billiards*, Russian Math. Surveys **45** (1990) 105–152.

[12] L. A. Bunimovich, Ya. G. Sinai and N. I. Chernov, *Statistical properties of two-dimensional hyperbolic billiards*, Russian Math. Surveys **46** (1991), 47–106.

[13] L. Bunimovich, H.-K. Zhang, and P. Zhang, *On another edge of defocusing: Hyperbolicity of asymmetric lemon billiards*, Commun. Math. Phys. **341** (2016), 781–803.

[14] N. I. Chernov, *Local ergodicity of hyperbolic systems with singularities*, Func. Anal. Appl. **27** (1993), 51–54.

[15] N. Chernov and R. Markarian, *Chaotic billiards*, Mathematical surveys and monographs Vol. 127, Amer. Math. Soc. (2006).

[16] N. Chernov and S. Troubetzkoy, *Ergodicity of billiards in polygons with pockets*, Nonlinearity **11** (1998), 1095–1102.

[17] A. Clarke and R. Ramírez-Ros, *Chaotic properties for billiards in circular polygons*, arXiv preprint arXiv:2309.09892 (2023).

[18] G. Del Magno and R. Markarian, *On the Bernoulli property of planar hyperbolic billiards*, Commun. Math. Phys. **350** (2017), 917–955.

[19] C. I. Delman and G. Galperin, *Billiards with pockets: A separation principle and bound for the number of orbit types*, Commun. Math. Phys. **230** (2002), 463–483.

[20] C. P. Dettmann and O. Georgiou, *Quantifying intermittency in the open drivebelt billiard*, Chaos, **22** (2012), 026113.

[21] B. Dietz, B. Mößner, T. Papenbrock, U. Reif and A. Richter *Bouncing ball orbits and symmetry breaking effects in a three-dimensional chaotic billiard*, Phys. Rev. E **77** (2008), 046221.

[22] V. J. Donnay, *Using integrability to produce chaos: billiards with positive entropy*, Commun. Math. Phys. **141** (1991), 225–257.

[23] R. Douady, *Applications du théoreme des tores invariants*, These de 3eme cycle (Doctoral dissertation, PhD thesis, Université Paris VII, 1982).

[24] G. Galperin, T. Krüger and S. Troubetzkoy, *Local instability of orbits in polygonal and polyhedral billiards*, Commun. Math. Phys. **169** (1995), 463–473,

[25] T. Gilbert and D. P. Sanders *Stable and unstable regimes in higher-dimensional convex billiards with cylindrical shape*, New J. Phys. **13** (2011), 023040.

[26] B. Halpern, *Strange billiard tables*, Trans. Amer. Math. Soc. **232** (1977), 297–305.

[27] A. Hassell and L. Hillairet, *Ergodic billiards that are not quantum unique ergodic*, Ann. of Math. (2) **171** (2010), 605–618.

[28] R. Markarian, *Billiards with Pesin region of measure one*, Commun. Math. Phys. **118** (1988), 87–97.

[29] D. Phillips, *Periodic billiard orbits in rounded triangles* Undergraduate project, University of Bristol (2016).

[30] R. E. Schwartz, *Obtuse triangular billiards II: One hundred degrees worth of periodic trajectories*, Exp. Math. **18** (2009) 137–171.

[31] D. Szász, *On the K-property of some planar hyperbolic billiards*, Commun. Math. Phys. **145** (1992) 595–604.

[32] M. Wojtkowski, *Principles for the design of billiards with nonvanishing Lyapunov exponents*, Commun. Math. Phys. **105** (1986), 391–414.

(C. P. Dettmann) University of Bristol, School of Mathematics, Fry building, Woodland Road, Bristol BS8 1TW, United Kingdom

Email address: `Carl.Dettmann@bristol.ac.uk`